Iranian Journal of Numerical Analysis and Optimization
Vol. 13, No. 1, 2023, pp 38–58
https://doi.org/10.22067/ijnao.2022.75413.1107
https://ijnao.um.ac.ir/

How to cite this article
Research Article

A modified Liu-Storey scheme for nonlinear systems with an application to image recovery

A.I. Kiri, M.Y. Waziri*, and K. Ahmed

Abstract

Like the Polak-Ribière-Polyak (PRP) and Hestenes-Stiefel (HS) methods, the classical Liu-Storey (LS) conjugate gradient scheme is widely believed to perform well numerically. This is attributed to the in-built capability of the method to conduct a restart when a bad direction is encountered. However, the scheme's inability to generate descent search directions, which is vital for global convergence, represents its major shortfall. In this article, we present an LS-type scheme for solving system of monotone nonlinear equations with convex constraints. The scheme is based on the approach by Wang et al. (2020) and the projection scheme by Solodov and Svaiter (1998). The new scheme satisfies the important condition for global convergence and is suitable for non-smooth nonlinear problems. Furthermore, we demonstrate the method's application in restoring blurry images in compressed sensing. The scheme's global convergence is established under mild assumptions and preliminary numerical results show that the proposed method is promising and performs better than two recent methods in the literature.

AMS subject classifications (2020): Primary 90C30; Secondary 90C26, 94A12.

*Corresponding author

Received 9 January 2022; revised 18 May 2022; accepted 19 May 2022

Aliyu Ibrahim Kiri
Department of Mathematical Sciences, Bayero University, Kano, Nigeria. e-mail: aikiri.mth@buk.edu.ng

Mohammed Yusuf Waziri
Department of Mathematical Sciences, Bayero University, Kano, Nigeria. e-mail: mywaziri.mth@buk.edu.ng

Kabiru Ahmed
Department of Mathematical Sciences, Bayero University, Kano, Nigeria. e-mail: kabiruhungu16@gmail.com

Keywords: Nonlinear Monotone Equations; Line search; Projection method; Signal processing; Convex constraint; Image de-blurring.

1 Introduction

In this paper, the following constrained system of nonlinear equations is considered:

$$F(x) = 0, \quad x \in \Phi, \tag{1}$$

where $F : \mathbf{R^n} \to \mathbf{R^n}$ is a nonlinear mapping, which is continuous and monotone, namely it satisfies the inequality

$$(F(x) - F(y))^T (x - y) \geq 0, \quad \forall x, y \in \mathbf{R^n}. \tag{2}$$

Also, Φ in (1) is nonempty, closed convex set, which is sometimes expressed as

$$\Phi = \{x \in \mathbf{R}^n : u \leq x \leq v\}, \tag{3}$$

where u and v stand for the lower and upper bounds on the vector x. Moreover, when Φ is expressed as (3), the problem in (1) is refereed to as box constrained nonlinear system.

Several applications in science, engineering and other areas of human endeavour involve the system of equations represented in (1). For example, in problem of radiactive transfer and transport theory [15], the popular Chanrasekhar integral equations is discretized and expressed as (1). Also, the economic equilibrium problems studied in [5, 24], are reformulated as problem (1). In addition, some $\ell_1 - norm$ regularized optimization problems in signal and image processing [23, 46] are obtained by reformulating systems of monotone nonlinear equations.

In order to solve (1), various iterative schemes have been proposed over the years. Newton-type schemes [32] and their improved variants, the quasi-Newton schemes [4, 17] are the most widely used due to their rapid convergence properties. These methods, however, are not suitable for large-dimension problems due to their huge matrix storage requirement. The conjugate gradient (CG) method, by virtue of its low memory requirement is the proper choice for problems with large dimensions. The scheme was primarily developed to solve the unconstrained optimization problem

$$\min_{x \in \mathbf{R}^n} f(x), \tag{4}$$

where $f : \mathbf{R}^n \longrightarrow \mathbf{R}$ denotes a nonlinear mapping that is assumed to be at least twice continuously differentiable and bounded below. The following notations are used with respect to problem (4):

$$g_k = g(x_k) = \nabla f(x_k), \quad g_{k-1} = g(x_{k-1}), \quad y_{k-1} = g_k - g_{k-1}.$$

The scheme is implemented using the iterative formula

$$x_0 \in \mathbf{R}^n, \quad x_{k+1} = x_k + s_k, \quad s_k = \alpha_k d_k, \quad k = 0, 1, ..., \tag{5}$$

where x_k denotes the k^{th} iterate, α_k represents a step-size that is computed using an appropriate line search technique, and d_k is the CG search direction defined by

$$d_k = -g_k + \beta_k d_{k-1}, \quad d_0 = -g_0, \tag{6}$$

and β_k is a scalar known as the CG (update) parameter, which defines each CG scheme and influences its performance. As part of the conditions for the sequence of iterative points $\{x_k\}$ generated via (5) and (6) to converge globally, the following sufficient descent condition is required:

$$d_k^T g_k \leq -\tau \|g_k\|^2, \quad \tau > 0. \tag{7}$$

Due to the fine attributes of CG methods with the known fact that the first order optimality condition for (4), namely, $\nabla f(x) = 0$, is equivalent to (1) with $F = \nabla f$ denoting the gradient of some nonlinear functions, different adaptations of the scheme for solving (1) have been proposed over the years. Search directions of these adaptations are defined as

$$d_k = \begin{cases} -F_k, & \text{if} \quad k = 0; \\ -F_k + \beta_k d_{k-1}, & \text{otherwise}, \end{cases} \tag{8}$$

where $F_k = F(x_k)$.

One of the CG adaptations that has gained attention of researchers in the last decade is the three-term methods for solving (1). Wang et al. [35], proposed a self-adaptive three-term nonlinear CG method for solving convex constrained system of nonlinear equations. Search direction of the scheme was obtained by employing an adaptive technique and under mild conditions, its global convergence was established. Based on the hyperplane projection scheme [32], Gao and He [9], proposed a three-term modified CG method for solving (1). Due to its derivative-free and low storage requirement, the method is also ideal for nonsmooth nonlinear problems. Motivated by the works in [1, 13, 27, 47], Koorapetse and Kaelo [25] also proposed three-term adaptation of CG projection methods for solving (1). The proposed methods were proven to satisfy the global convergence condition and under suitable assumptions, the authors showed that the schemes converge globally. For more details see ([44, 37, 38, 39, 40, 31, 41, 11, 42, 10, 43, 12, 33, 26]).

In this paper, our aim is to develop an efficient three-term adaptation of the Liu-Storey (LS) [22] CG method for solving (1). Our inspiration comes from the work of Wang et al. [36] and the projection method by Solodov and Svaiter [32]. Apart from developing a new scheme that satisfies the condition for global convergence, a notable contribution of this research is its application in restoring blurry images, which is a trend in compressed sensing.

The paper is organized as follows: Some preliminaries leading to derivation of the proposed method are given in Section 2. The proposed method and its convergence analysis are presented in Section 3. Numerical results and their discussions are presented in Section 4, while application of the proposed scheme is discussed in Section 5. Concluding remarks are made in Section 6.

2 Preliminaries

In the remaining part of the article, $\|x\| = \sqrt{x^T x}$, stands for the ℓ_2 *norm*, $F_{k-1} = F(x_{k-1})$, and $s_{k-1} = x_k - x_{k-1}$. The following assumptions will be required later in the article:

(i) The solution set Φ is not empty, namely, there exists $\tilde{x} \in \Phi$ such that $F(\tilde{x}) = 0$.

(ii) The mapping F satisfies the Lipschitz continuity property; i.e, there exists a positive constant L such that for all $x, y \in \mathbf{R}^n$, the following is satisfied:

$$\|F(x) - F(y)\| \leq L\|x - y\|. \tag{9}$$

We now introduce the projection operator. Let $\Phi \subset \mathbf{R}^n$ be a nonempty, closed and convex set. Then for each vector $x \in \mathbf{R}^n$, its projection onto Φ is given by

$$P_\Phi(x) = \arg\min \|x - y\| : y \in \Phi.$$

$P_\Phi : \mathbf{R}^n \to \Phi$ is referred to as the projection operator, with the nonexpansive property given by,

$$\|P_\Phi(x) - P_\Phi(y)\| \leq \|x - y\|, \quad \forall x, y \in \mathbf{R}^n,$$

for which, we can write

$$\|P_\Phi(x) - y\| \leq \|x - y\|, \quad \forall y \in \Phi. \tag{10}$$

3 Motivation, algorithm and global convergence of the new method

This section deals with motivation of the scheme, its algorithm and convergence analysis. First, we introduce the spectral CG method, which is an extension of the classical scheme for solving (4). By employing the spectral gradient scheme by Barzilai and Bowein [2], Birgin and Martinez [3] developed a spectral CG (SCG) method with the following search direction:

$$d_k = -\theta_k g_k + \beta_k d_{k-1},$$

where the update parameter β_k is defined by

$$\beta_k = \frac{(\theta_k y_{k-1} - s_{k-1})^T g_k}{d_{k-1}^T y_{k-1}},$$

and θ_k is the spectral parameter given as

$$\theta_k = \frac{s_{k-1}^T s_{k-1}}{s_{k-1}^T y_{k-1}}.$$

The scheme is computationally efficient, but its search directions are generally not descent directions, i.e, the scheme does not satisfy the inequality defined in (7). Over the years, three-term SCG schemes that satisfy the condition (7) have been developed. By modifying the classical PRP CG method [29, 30], Li et al. [21] proposed a spectral three-term scheme with the following search direction:

$$d_k = \begin{cases} -\gamma_k g_k + \beta_k^{MPRP} d_{k-1} - v_k y_{k-1} & k \geq 1; \\ -g_k, & \text{if} \quad k = 0, \end{cases}$$

with

$$\beta_k^{MPRP} = \frac{g_k^T y_{k-1}}{\varphi |g_k^T d_{k-1}| + \|g_{k-1}\|^2}, \quad v_k = \frac{g_k^T d_{k-1}}{\varphi |g_k^T d_{k-1}| + \|g_{k-1}\|^2}, \quad \varphi \geq 0.$$

Simple inspection reveals that the method satisfies the sufficient descent condition (7). Also, by employing standard assumptions, the authors proved global convergence of the scheme for uniformly convex functions. Only recently, Wang et al. [36] presented a spectral three-term modification of the classical Conjugate Descent scheme [8] with search direction defined as

$$d_k = \begin{cases} -\gamma_k g_k + \frac{\|g_k\|^2 d_{k-1} - (g_k^T d_{k-1}) g_k}{\max\{-d_{k-1}^T g_{k-1}, \eta_1 \|g_k\| \|d_{k-1}\|\}} & k \geq 1; \\ -g_k, & \text{if} \quad k = 0, \end{cases}$$

where

$$\gamma_k = \frac{\phi_k}{\min\{\eta_2 s_{k-1}^T y_{k-1}, \eta_3 \phi_k\}}, \quad \phi_k = \|s_{k-1}\|^2, \quad \eta_1 > 0, \quad \eta_2, \eta_3 \in (0,1).$$

Now, like the classical PRP [29, 30] and HS [14] methods, the classical LS [22] CG scheme is equipped with an in-built mechanism that addresses the jamming phenomenon. So, like the others in the group, the scheme is numerically effective. However, it does not satisfy the sufficient descent condition (7). Motivated by this shortcoming of the LS scheme, the nice attributes of three-term methods discussed above and the spectral three-term scheme by Wang et al. [36], we propose a spectral three-term adaptation of the LS scheme [22] with the following search direction:

$$d_k = \begin{cases} -\gamma_k F_k + \frac{F_k^T \bar{y}_{k-1} d_{k-1} - F_k^T d_{k-1} \bar{y}_{k-1}}{\max\{-d_{k-1}^T F_{k-1}, \zeta_1 \|\bar{y}_{k-1}\| \|d_{k-1}\|\}} & k \geq 1; \\ -F_k, & \text{if} \quad k = 0, \end{cases} \tag{11}$$

where

$$\gamma_k = \frac{\max\{\zeta_2 \|s_{k-1}\|^2, \zeta_3 \chi_k\}}{\chi_k}, \; \chi_k = s_{k-1}^T \bar{y}_{k-1}, \quad \zeta_1 > 0, \quad \zeta_2, \zeta_3 \in (0,1), \tag{12}$$

and

$$\bar{y}_{k-1} = y_{k-1} + r s_{k-1}, \quad y_{k-1} = F_k - F_{k-1}, \quad r > 0.$$

Note: It can easily be deduced from (11) and (12) that

$$\max\{-d_{k-1}^T F_{k-1}, \zeta_1 \|\bar{y}_{k-1}\| \|d_{k-1}\|\} \geq \zeta_1 \|\bar{y}_{k-1}\| \|d_{k-1}\|, \tag{13}$$

and

$$\frac{\max\{\zeta_2 \|s_{k-1}\|^2, \zeta_3 \chi_k\}}{\chi_k} \geq \frac{\zeta_3 \chi_k}{\chi_k} = \zeta_3. \tag{14}$$

Next, we obtain a bound for the spectral parameter γ_k. To achieve that, we analyze two cases:

First case: If $\max\{\zeta_2 \|s_{k-1}\|^2, \zeta_3 \chi_k\} = \zeta_2 \|s_{k-1}\|^2$, then, by monotonicity of F, and definition of $\bar{y}_{k-1}$, we have

$$s_{k-1}^T \bar{y}_{k-1} = s_{k-1}^T y_{k-1} + r \|s_{k-1}\|^2 \geq r \|s_{k-1}\|^2. \tag{15}$$

So, using (15) we have that

$$\gamma_k = \frac{\max\{\zeta_2 \|s_{k-1}\|^2, \zeta_3 \chi_k\}}{\chi_k} = \frac{\zeta_2 \|s_{k-1}\|^2}{s_{k-1}^T \bar{y}_{k-1}} \leq \frac{\zeta_2 \|s_{k-1}\|^2}{r \|s_{k-1}\|^2} = \frac{\zeta_2}{r}.$$

Second case: If $\max\{\zeta_2 \|s_{k-1}\|^2, \zeta_3 \chi_k\} = \zeta_3 \chi_k$, then

$$\gamma_k = \frac{\max\{\zeta_2 \|s_{k-1}\|^2, \zeta_3 \chi_k\}}{\chi_k} = \frac{\zeta_3 \chi_k}{\chi_k} = \zeta_3.$$

Therefore, setting $\kappa = \max\{\frac{\zeta_2}{r}, \zeta_3\}$, we see that $0 < \gamma_k \leq \kappa$.

Algorithm 1. Modified Liu-Storey Method (MLSTM)

Step 0: Choose a tolerance $\epsilon > 0$, initial guess $x_0 \in \Phi$, $\beta > 0, \rho \in (0,1)$, $0 < \varsigma < 2$, $\sigma > 0$. Set $k = 0$ and $d_0 = -F_0$.

Step 1: Compute $F(x_k)$. If $\|F(x_k)\| \leq \epsilon$, stop, if not, proceed to **Step** 2.

Step 2: Find $z_k = x_k + t_k d_k$, where

$$t_k = \max\{\beta\rho^m : m = 0, 1, 2, ...\},$$

for which

$$-F(x_k + t_k d_k)^T d_k \geq \sigma t_k \|d_k\|^2, \tag{16}$$

Step 3: If $z_k \in \Phi$ and $\|F(z_k)\| \leq \epsilon$ stop, else determine

$$x_{k+1} = P_\Phi\left[x_k - \varsigma \mu_k F(z_k)\right], \tag{17}$$

where

$$\mu_k = \frac{F(z_k)^T(x_k - z_k)}{\|F(z_k)\|^2}. \tag{18}$$

Step 4: Obtain the direction d_{k+1} by (11) and (12).

Step 5: Set $k = k + 1$. Go to **Step** 1.

Lemma 1. Let the sequence $\{d_k\}$ be generated by (11) and (12). Then

$$F_k^T d_k \leq -\tau \|F_k\|^2, \quad \tau > 0. \tag{19}$$

Proof. First, from (14) we have that $\gamma_k \geq \zeta_3$. This implies that $-\gamma_k \leq -\zeta_3$. We now consider two cases:

1. For $k = 0$, by (11), it is obvious that $F_0^T d_0 = -\|F_0\|^2$.

2. For $k \geq 1$, from (11) and (12), we have

$$\begin{aligned} F_k^T d_k &= -\gamma_k \|F_k\|^2 + \frac{(F_k^T \bar{y}_{k-1}) d_{k-1}^T F_k - (d_{k-1}^T F_k) F_k^T \bar{y}_{k-1}}{\max\{-d_{k-1}^T F_{k-1}, \zeta_1 \|\bar{y}_{k-1}\| \|d_{k-1}\|\}} \\ &= -\gamma_k \|F_k\|^2 \\ &\leq -\zeta_3 \|F_k\|^2. \end{aligned} \tag{20}$$

Setting $\tau = \zeta_3$, we obtain the result in both cases. □

In the following Lemma, we prove that when the solution of (1) is not attained, i.e., $F(x) \neq 0$, then a stepsize t_k exists for which (16) is satisfied.

Lemma 2. Suppose condition (i) in section 2 holds. Then, for every $k \geq 0$, there exists a positive constant t_k such that (16) is satisfied.

Proof. Assuming that the statement is not true. It implies that a constant k_0 exists for which (16) does not hold for each integer $m \geq 0$, namely

$$-F(x_{k_0} + \beta\rho^m d_{k_0})^T d_{k_0} < \sigma\beta\rho^m \|d_{k_0}\|^2.$$

By employing the continuity of F with the fact that $\rho \in (0, 1)$, letting the integer m grow to infinity namely, $m \to \infty$, we obtain

$$-F(x_{k_0})^T d_{k_0} \leq 0. \tag{21}$$

From (19), we have

$$-F(x_{k_0})^T d_{k_0} \geq \tau \|F(x_{k_0})\|^2 > 0. \tag{22}$$

Clearly (21) and (22) do not agree. So, a contradiction is obtained, which establishes the proof. □

Lemma 3. Let the sequences $\{x_k\}$ and $\{z_k\}$ be generated by Algorithm 1, then

$$t_k \geq \min\left\{\beta, \frac{\rho\tau\|F_k\|^2}{(L+\sigma)\|d_k\|^2}\right\}. \tag{23}$$

Proof. By (16), we see that if $t_k = \beta$, then (16) is satisfied. Conversely, if $t_k \neq \beta$ then $\bar{t}_k = \frac{t_k}{\rho}$ will not satisfy (16), i.e.,

$$-F(x_k + \frac{t_k}{\rho} d_k)^T d_k < \sigma \frac{t_k}{\rho} \|d_k\|^2. \tag{24}$$

By Assumption (ii) and (19), we can write

$$\begin{aligned}
\tau\|F_k\| &\leq -F_k^T d_k \\
&= (F(x_k + \frac{t_k}{\rho} d_k) - F(x_k))^T d_k - F(x_k + \frac{t_k}{\rho} d_k)^T d_k \\
&\leq L\frac{t_k}{\rho}\|d_k\|^2 - \sigma\frac{t_k}{\rho}\|d_k\|^2 \\
&= \frac{t_k}{\rho}(L+\sigma)\|d_k\|^2,
\end{aligned} \tag{25}$$

which ultimately yields the desired inequality and the proof is completed. □

Lemma 4. Let conditions (i) and (ii) in section 2 hold. Then the sequences $\{x_k\}$ and $\{z_k\}$ generated by Algorithm 1 are bounded and

$$\lim_{k\to\infty} t_k \|d_k\| = 0. \tag{26}$$

Proof. First, we prove boundedness of the sequences $\{x_k\}$ and $\{z_k\}$. Let $\tilde{x} \in \Phi$ be a solution of (1). Then by (2), we have

$$\begin{aligned}
(x_k - \tilde{x})^T F(z_k) &= (x_k - z_k + z_k - \tilde{x})^T F(z_k) \\
&= (x_k - z_k)^T F(z_k) + (z_k - \tilde{x})^T F(z_k) \\
&\geq (x_k - z_k)^T F(z_k) + (z_k - \tilde{x})^T F(\tilde{x}) \\
&= (x_k - z_k)^T F(z_k).
\end{aligned} \tag{27}$$

Also from (10), (18), and the fact that $0 < \varsigma < 2$, we have

$$\begin{aligned}\|x_{k+1}-\tilde{x}\|^2 &= \|P_\Phi(x_k-\varsigma\mu_k F(z_k))-\tilde{x}\|^2\\ &\le \|x_k-\varsigma\mu_k F(z_k)-\tilde{x}\|^2\\ &= \|(x_k-\tilde{x})-\varsigma\mu_k F(z_k)\|^2\\ &= \|x_k-\tilde{x}\|^2-2\varsigma\mu_k F(z_k)^T(x_k-\tilde{x})+\varsigma^2\mu_k^2\|F(z_k)\|^2\\ &\le \|x_k-\tilde{x}\|^2-2\varsigma\mu_k F(z_k)^T(x_k-z_k)+\varsigma^2\mu_k^2\|F(z_k)\|^2\\ &= \|x_k-\tilde{x}\|^2-\varsigma(2-\varsigma)\frac{(F(z_k)^T(x_k-z_k))^2}{\|F(z_k)\|^2}\\ &\le \|x_k-\tilde{x}\|^2,\end{aligned} \tag{28}$$

which consequently yields

$$\|x_{k+1}-\tilde{x}\| \le \|x_k-\tilde{x}\|, \quad \forall k \ge 0. \tag{29}$$

And in a recursive manner, (29) implies that $\|x_k-\tilde{x}\| \le \|x_0-\tilde{x}\|$. So, the sequence $\{\|x_k-\tilde{x}\|\}$ is decreasing and convergent, which means that $\{x_k\}$ is bounded. Also, by assumption (i), (9) and (29) we have

$$\|F(x_k)\| = \|F(x_k)-F(\tilde{x})\| \le L\|x_k-\tilde{x}\| \le L\|x_0-\tilde{x}\|.$$

Setting $L\|x_0-\tilde{x}\| = \pi$, we obtain that

$$\|F(x_k)\| \le \pi. \tag{30}$$

Also, from (16) and definition of z_k, we get

$$F(z_k)^T(x_k-z_k) = -t_k F(z_k)^T d_k \ge \sigma t_k^2\|d_k\|^2 = \sigma\|x_k-z_k\|^2. \tag{31}$$

By employing (2) and the Cauchy-Schwartz inequality, we can write

$$\begin{aligned}F(z_k)^T(x_k-z_k) &= (F(z_k)-F(x_k))^T(x_k-z_k)+F(x_k)^T(x_k-z_k)\\ &\le \|F(x_k)\|\|x_k-z_k\|.\end{aligned} \tag{32}$$

By (30),(31) and (32) we can write

$$\sigma\|x_k-z_k\|^2 \le \|F(x_k)\|\|x_k-z_k\|,$$

which leads to

$$\|x_k-z_k\| \le \frac{\pi}{\sigma}.$$

Hence, the sequence $\{z_k\}$ is also bounded. Now, the boundedness of $\{z_k\}$, implies that $\{\|z_k-\tilde{x}\|\}$ is bounded, i.e., there exists $\pi_2 > 0$ such that for any $\tilde{x} \in \Phi$

$$\|z_k-\tilde{x}\| \le \pi_2. \tag{33}$$

Similarly, from (9) and (33), we have

$$\|F(z_k)\| = \|F(z_k) - F(\tilde{x})\| \leq L\|z_k - \tilde{x}\| \leq L\pi_2.$$

Hence, setting $\pi_3 = L\pi_2$, we obtain

$$\|F(z_k)\| \leq \pi_3. \tag{34}$$

Also, using (16), we have

$$\sigma^2 t_k^4 \|d_k\|^4 \leq t_k^2 (F(z_k)^T d_k)^2. \tag{35}$$

By combining (28) and (35), we obtain

$$\sigma^2 t_k^4 \|d_k\|\|^4 \leq \frac{\|F(z_k)\|^2}{\varsigma(2-\varsigma)}(\|x_k - \tilde{x}\|^2 - \|x_{k+1} - \tilde{x}\|^2). \tag{36}$$

Now, by (29) we have that the sequence $\{\|x_k - \tilde{x}\|\}$ is convergent, and also by (34) $\{F(z_k)\}$ is bounded. Hence, taking limits of both sides of (36) as k approaches infinity, we have

$$\sigma^2 \lim_{k \to \infty} t_k^4 \|d_k\|^4 \leq 0,$$

which consequently leads to the desired result, i.e.,

$$\lim_{k \to \infty} t_k \|d_k\| = 0. \tag{37}$$

□

Lemma 5. Let the sequence of search directions $\{d_k\}$ be generated by Algorithm 1. Then $\{d_k\}$ is bounded, namely, a constant $\vartheta > 0$ exists such that

$$\|d_k\| \leq \vartheta, \quad \forall k \quad \text{positive}. \tag{38}$$

Proof. From (11), (13), (30), and the Cauchy-Schwartz inequality, we obtain

$$\begin{aligned}
\|d_k\| &= \left\| -\gamma_k F_k + \frac{F_k^T \bar{y}_{k-1} d_{k-1} - F_k^T d_{k-1} \bar{y}_{k-1}}{\max\{-d_{k-1}^T F_{k-1}, \zeta_1 \|\bar{y}_{k-1}\|\|d_{k-1}\|\}} \right\| \\
&\leq \gamma_k \|F_k\| + \frac{\|F_k\|\|\bar{y}_{k-1}\|\|d_{k-1}\| + \|F_k\|\|\bar{y}_{k-1}\|\|d_{k-1}\|}{\max\{-d_{k-1}^T F_{k-1}, \zeta_1 \|\bar{y}_{k-1}\|\|d_{k-1}\|\}} \\
&\leq \gamma_k \|F_k\| + \frac{2\|F_k\|\|\bar{y}_{k-1}\|\|d_{k-1}\|}{\zeta_1 \|\bar{y}_{k-1}\|\|d_{k-1}\|} \\
&= \gamma_k \|F_k\| + \frac{2\|F_k\|}{\zeta_1} \\
&\leq \left(\kappa + \frac{2}{\zeta_1}\right) \|F_k\|
\end{aligned}$$

$$\leq \left(\kappa + \frac{2}{\zeta_1}\right)\pi. \tag{39}$$

By setting $\vartheta = \left(\kappa + \frac{2}{\zeta_1}\right)\pi$, the proof is established. □

The following theorem establishes global convergence of Algorithm 1.

Theorem 1. Given that conditions (i) and (ii) hold. Consider the sequences $\{x_k\}$ and $\{z_k\}$ generated by Algorithm 1. Then

$$\liminf_{k\to\infty} \|F_k\| = 0.$$

Proof. For the proof, we assume that the conclusion is not true. Then it implies that a constant $\bar{c} > o$ exists for which

$$\|F_k\| \geq \bar{c}, \quad \forall k \geq 0. \tag{40}$$

Utilizing (19), (40) and Cauchy Schwartz inequality yields

$$\|d_k\| \geq \tau\bar{c}, \quad \forall k \geq 0. \tag{41}$$

Similarly, by employing the inequalities (23), (39), (40), (41), and for all k sufficiently large, we get

$$\begin{aligned} t_k\|d_k\| &\geq \min\left\{\beta, \frac{\rho\tau\|F_k\|^2}{(L+\sigma)\,\|d_k\|^2}\right\}\|d_k\| \\ &\geq \min\left\{\beta\tau\bar{c}, \frac{\rho\tau\bar{c}^2}{(L+\sigma)\,\vartheta}\right\} > 0. \end{aligned} \tag{42}$$

Clearly, the second inequality in (42) contradicts (37). Therefore, we conclude that $\liminf_{k\to\infty}\|F_k\| = 0$. □

4 Numerical experiments and discussions

Here, we investigate the effectiveness of Algorithm 1 by comparing its performance with the two methods presented in [16, 18]. The experiments with all the three algorithms were conducted using the backtracking line search (16). For the other two methods, which we label as $MLSCD$ and $HCGP$ for simplicity, we set the parameters as they are used in the respective papers. For Algorithm 1, we set $\rho = 0.6$, $\beta = 1$, $\sigma = 10^{-3}$, $\varsigma = 1.6, r = 1, \zeta_1 = 0.5, \zeta_2 = 0.5, \zeta_3 = 0.6$. Codes for the algorithms were written using Matlab $R2014a$ and run on a PC (2.30GHZ CPU, 4GB RAM). The iteration is set to stop for all the methods when the number of iterations exceed 1000 or whenever any of the following inequalities is satisfied:

$$\|F(x_k)\| \leq 10^{-8},$$

$$\|F(z_k)\| \leq 10^{-8}.$$

The following test problems were used to test the three methods.

Problem 4.1. This is a modification of the problem obtained from [34]. The mapping F takes the form $F(x) = (f_1(x), f_2(x), ..., f_n(x))^T$, where

$f_i(x) = (e^{x_i})^2 + 3\sin x_i - 1, \quad i = 2, \dots, n-1,$
with $\Phi = \mathbf{R}^n_+$.

Problem 4.2. Exponential Function II obtained from [19]. The mapping F takes the form $F(x) = (f_1(x), f_2(x), ..., f_n(x))^T$, where

$f_1(x) = e^{x_1} - 1, \quad i = 2, 3, \dots, n,$
$f_i(x) = \frac{i}{10}(e^{x_i} + x_{i-1} - 1),$
with $\Phi = \mathbf{R}^n_+$.

Problem 4.3. Non-smooth Function obtained from[20]. The mapping F takes the form $F(x) = (f_1(x), f_2(x), ..., f_n(x))^T$, where

$f_i(x) = 2x_i - \sin|x_i|, \quad i = 1, 2, \dots, n,$
with $\Phi = \left\{ x \in \mathbf{R}^n : \sum_{i=1}^{n} x_i \leq n, \quad x_i \geq 0, \quad i = 1, 2, \dots, n \right\}.$

Problem 4.4. Strictly Convex Function obtained from [34]. The mapping F takes the form $F(x) = (f_1(x), f_2(x), ..., f_n(x))^T$, where

$f_i(x) = e^{x_i} - 1, \quad i = 1, 2, \dots, n,$
with $\Phi = \mathbf{R}^n_+$.

Problem 4.5. Tridiagonal Exponential Function obtained from [23]. The mapping F takes the form $F(x) = (f_1(x), f_2(x), ..., f_n(x))^T$, where

$$f_1(x) = x_1 - e^{\left(cos\frac{x_1+x_2}{n+1}\right)},$$
$$f_i(x) = x_i - e^{\left(cos\frac{x_{i-1}+x_i+x_{i+1}}{n+1}\right)}, \quad i = 2, 3, \dots, n-1,$$
$$f_n(x) = x_n - e^{\left(cos\frac{x_{n-1}+x_n}{n+1}\right)}.$$

with $\Phi = \mathbf{R}^n_+$.

Problem 4.6. Non-smooth Function obtained from [46]. The mapping F takes the form $F(x) = (f_1(x), f_2(x), ..., f_n(x))^T$, where

$f_i(x) = x_i - \sin|x_i - 1|, \quad i = 1, 2, \dots, n,$
with $\Phi = \left\{ x \in \mathbf{R}^n : \sum_{i=1}^{n} x_i \leq n, \quad x_i \geq 0, \quad i = 1, 2, \dots, n \right\}.$

Problem 4.7 The problem is obtained from [19]. The mapping F takes the form $F(x) = (f_1(x), f_2(x), ..., f_n(x))^T$, where

$f_1(x) = e^{x_1} - 1,$
$f_i(x) = e^{x_i} + x_{i-1} - 1, \quad i = 2, \ldots, n-1,$
with $\Phi = \mathbf{R}^n_+$.

Problem 4.8 Modified version of the non-smooth Function in Problem 4.6. The mapping F takes the form $F(x) = (f_1(x), f_2(x), ..., f_n(x))^T$, where

$f_i(x) = x_i - 2\sin|x_i - 1|, \quad i = 1, 2, \ldots, n,$

with $\Phi = \left\{ x \in \mathbf{R}^n : \sum_{i=1}^{n} x_i \leq n, \quad x_i \geq 0, \quad i = 1, 2, \ldots, n \right\}.$

For each of the above test functions, 24 numerical experiments were performed with variables 1000, 10,000 50,000, and the following starting points:

$x_0^1 = (1, 1, ..., 1)^T, x_0^2 = (2, 2, ..., 2)^T, x_0^3 = (3, 3, ..., 3)^T, x_0^4 = (4, 4, ..., 4)^T,$
$x_0^5 = (5, 5, ..., 5)^T, x_0^6 = (6, 6, ..., 6)^T, x_0^7 = (7, 7, ..., 7)^T, x_0^8 = (8, 8, ..., 8)^T,.$

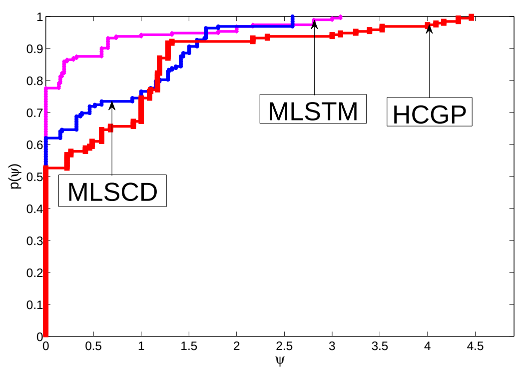

Figure 1: Performance profile with respect to number of iterations

Furthermore, we adopt Dolan and Moré [6] performance profile in order to present a graphical view of the performance of each of the three schemes considered in the experiments. In line with this, three figures were plotted with respect to three performance metrics, namely, number of iterations, function evaluations and processing time. For each figure, the $vertical - axis$ corresponds to the percentage of the problems solved by any one of the algorithms with the least value of any of the metric under consideration; the right side, represents the percentage of problems solved successfully by each algorithm. Also, the topmost curve in each figure corresponds to the algorithm that solved the most problems in the experiments. It can be observed from Fig. 1, that the $MLSTM$ algorithm solved 78% of problems with least number of iterations compared to the $MLSCD$ and $HCGP$ algorithms that recorded 62% and 54% respectively. We have to note here, that this percentage values as shown in the figure, represent sums of the percentages recorded by each algorithm with least number of iterations and the ties recorded for

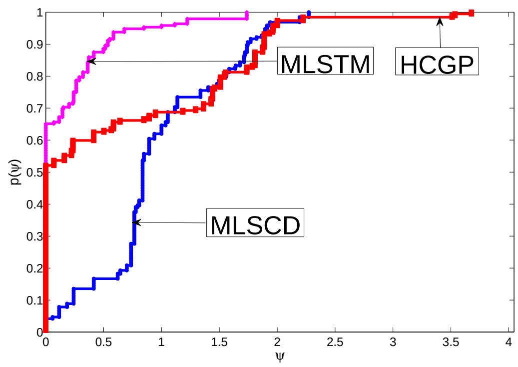

Figure 2: Performance profile with respect to function evaluation

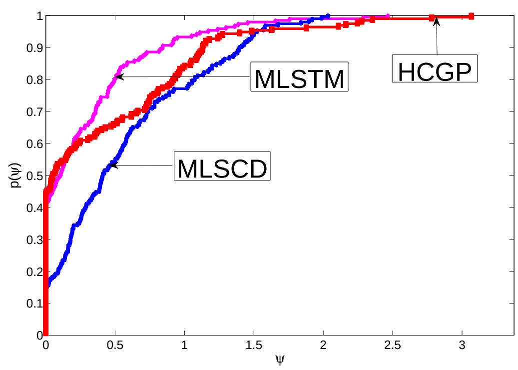

Figure 3: Performance profile with respect to CPU time

the same metric. From Fig. 2 it is observed that the $MLSTM$ algorithm solved 65% of the problems with least function evaluations compared to the $HCGP$ and $MLSCD$ algorithms that recorded 52% and 4% respectively. As in the earlier case, here too the percentage values are sums of the values recorded by each algorithm with least function values and the ties it recorded with any one or two other algorithms. Based on least processing time metric, Fig. 3 indicated that the $HCGP$ algorithm has an edge over the $MLSTM$ and $MLSCD$ algorithms as it solved 45% of the problems with minimum processing time, while the other two algorithms recorded 40% and 18% respectively. Moreover, it is observed that the topmost curve in all the three figures corresponds to the $MLSTM$ algorithm. Hence, considering the graphical representations in Figs 1, 2, and 3, and the above analysis, it can be concluded that the $MLSTM$ algorithm is more effective for solving the problem represented in (1) than the $MLSCD$ and $HCGP$ algorithms.

5 Application of the proposed scheme

Obtaining sparse solutions to ill-conditioned linear systems of equations is the interest in most signal and image processing problems. Typically, this involves minimizing the following $\ell_1 - \ell_2$ *norm* problem

$$\min_x \frac{1}{2}\|Hx - w\|_2^2 + \delta\|x\|_1, \tag{43}$$

where δ is a nonnegative parameter, $x \in \mathbf{R}^n, w \in \mathbf{R}^k$ is an observed value, $H \in \mathbf{R}^{k\times n}(k < n)$ denotes a linear mapping, while $\|x\|_1$ and $\|x\|_2$ represents the ℓ_1 and ℓ_2 *norms* respectively. Clearly, (43) represents a convex unconstrained optimization problem.

In order to solve (43), Figueiredo et al. [7] reformulated it as a convex quadratic problem, where each vector $x \in \mathbf{R}^n$ is split into two parts and written as

$$x = a - b, \quad a \geq 0, \quad b \geq 0, \quad a, b \in \mathbf{R}^n. \tag{44}$$

with $a_i = (x_i)_+, b_i = (-x_i)_+, \forall i = 1, 2, ..., n$ and $(.)_+ = \max\{0, x\}$. Applying the above representation to (43), we obtain

$$\min_{a,b} \frac{1}{2}\|H(a - b) - w\|_2^2 + \delta e_n^T a + \delta e_n^T b, \tag{45}$$

where $e_n = (1, 1, ..., 1)^T \in \mathbf{R}^n$. Going by Figueiredo et al. [7], the problem in (45) is reformulated as

$$\min_z \frac{1}{2}z^T Az + D^T z, \quad z \geq 0, \tag{46}$$

which is a quadratic program problem with

$$z = \begin{pmatrix} a \\ b \end{pmatrix}, \quad D = \delta e_{2n} + \begin{pmatrix} -y \\ y \end{pmatrix}, \quad y = H^T w, \quad A = \begin{pmatrix} H^T H & -H^T H \\ -H^T H & H^T H \end{pmatrix}. \tag{47}$$

In [45], the quadratic program problem in (46) was reformulated and shown to be equivalent to

$$F(z) = \min\{z, Az + D\} = 0, \tag{48}$$

where F represents a vector-valued mapping. Also, since F is monotone and Lipschitz continuous (see [28, 45]), the $MLSTM$ scheme can conveniently be applied to solve it.

5.1 Image restoration experiment

Here, we conduct some experiments with the $MLSTM$ scheme to further demonstrate its effectiveness and application in image reconstruction. For the experiments, four images are employed, which includes *Barbera*, *Lena*, *Einstein*, and *Cameraman*. As in the previous experiments, all codes are generated on MATLAB $R2014a$ with the same configuration and parameter values set as applied in the earlier experiments. Also, we test performance of the $MLSTM$ method with the $CGDESCENT$ [46] solver, which is used in image restoration problems. The same values of the parameters used by the author were also applied in the experiments. The performance of both schemes are compared in terms of final objective function value (Obj), mean square error (MSE), signal to noise ratio (SNR), which is given by

$$SNR = 20 \times \log_{10} \left(\frac{\|x\|}{\|\tilde{x} - x\|} \right),$$

and the structural similarity index (SSIM), which computes the similarity between original image and the restored one in each of the experiments conducted. Results of the experiments conducted are presented in table 1, while Fig. 4 displays the original, blurred, and reconstructed images obtained by the $MLSTM$ and $CGDESCENT$ schemes. Fig. 4 reveals that the quality of reconstructed images by the $MLSTM$ method for all the images considered, is somewhat better than that of $CGDESCENT$ scheme. Also, table 1 showed that the $MLSTM$ algorithm performed much better regarding Obj, MSE, SNR and SSIM metrics than the $CGDESCENT$ scheme. However, the $CGDESCENT$ scheme is much faster as it recorded less processing time than the $MLSTM$ algorithm. Hence, going by these results, it can be concluded that the $MLSTM$ algorithm is promising for reconstruction of the images considered.

Table 1: Image restoration results for MLSTM and CGDESCENT

IMAGE	SIZE	MLSTM					CGDESCENT				
		Obj	MSE	SNR	PT	SSIM	Obj	MSE	SNR	PT	SSIM
BARBERA	256×256	1.523×10^6	1.5267×10^2	20.85	10.75	0.80	1.585×10^6	2.0627×10^2	19.55	1.45	0.75
LENA	256×256	1.448×10^6	6.4566×10^1	24.37	17.81	0.90	1.513×10^6	9.0025×10^1	22.93	1.81	0.87
EINSTEIN	256×256	1.012×10^6	7.0780×10^1	21.39	10.33	0.86	1.045×10^6	8.7884×10^1	20.45	3.59	0.83
CAMERAMAN	256×256	1.430×10^6	1.4128×10^2	21.05	9.59	0.85	1.47×10^6	1.78×10^2	20.05	3.14	0.83

6 Conclusion

An efficient modified Liu-Storey scheme ($MLSTM$) for solving constrained system of monotone nonlinear equations was presented in this article. The

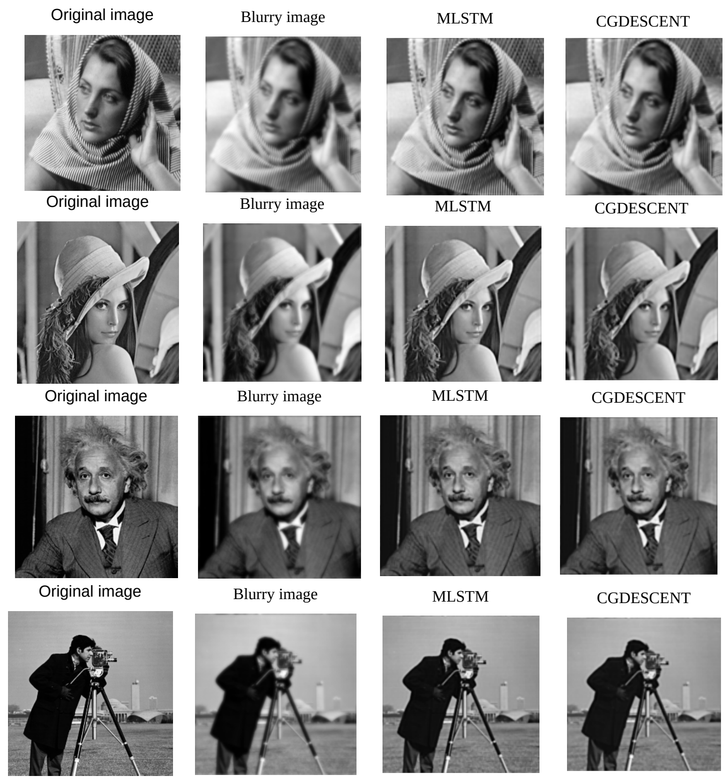

Figure 4: Original and blurred images (First and second columns from the left). Restored images by MLSTM and CGDESCENT methods (last two columns).

scheme is ideal for large dimension problems as well as non-smooth functions because it avoids computing derivatives and requires less memory to implement. Apart from inheriting numerical efficiency of the classical LS scheme, the new method satisfies the important condition for global convergence. The scheme's global convergence was established by employing basic assumptions. Also, numerical experiments conducted with some test problems indicate that the proposed scheme is promising as it is competitive and more efficient compared to the $MLSCD$ and $HCGP$ methods in [16, 18]. Furthermore, an interesting novelty of the scheme is its application to solving the regularized ℓ_1 $norm$ problem in compressed sensing. By conducting some experiments to recover blurry images, the scheme proved to be effective as it competes with and produces better results than the popular $CGDESCENT$ scheme in

[46]. As a further research, we intend to explore application of the $MLSTM$ scheme and its modified version to other area of interest.

Conflict of Interest The authors declare that they have no conflict of interest.

Acknowledgements The authors are grateful for the helpful and constructive comments by the anonymous reviewers and editors.

References

[1] Ahookhosh, M. Amini, K. and Bahrami, S. *Two derivative-free projection approaches for systems of large-scale nonlinear monotone equations*, Numer. Algor. 64(2013), 21-42.

[2] Barzilai, J. and Borwein, J.M. *Two point step size gradient method*, IMA J. Numer. Anal. 8(1988),141-148.

[3] Birgin, E.G. and Martinez, J.M. *A spectral conjugate gradient method for unconstrained optimization*, Appl. Math. Optim. 43 (2001), 117-128.

[4] Dennis, J. and Moré, J. *Quasi-Newton methods, motivation and theory*, SIAM Review, Soc. Ind. Appl. Math. 19(1)(1977), 46-89.

[5] Dirkse, S.P. and Ferris, M.C. *A collection of nonlinear mixed complementarity problems*, Optim. Methods Softw. 5(1995)319-345.

[6] Dolan, E.D. and Moré, J.J. *Benchmarking optimization software with performance profiles*, Math. Program. 91(2002), 201-2013.

[7] Figueiredo, M. Nowak, R. and Wright, S.J. *Gradient projection for sparse reconstruction, application to compressed sensing and other inverse problems*, IEEE J-STSP IEEE Press, Piscataway, NJ. (2007), 586-597.

[8] Fletcher, R. *Practical method of Optimization*, Volume 1: Unconstrained Optimization, 2nd ed., Wiley, New York, 1997

[9] Gao, P. and He, C. *An efficient three-term conjugate gradient method for nonlinear monotone equations with convex constraints*, Calcolo 55(53)(2018),1-17.

[10] Halilu, A.S. Majumder, A. Waziri, M.Y. Awwal, A.M. and Ahmed, K. *On solving double direction methods for convex constrained monotone nonlinear equations with image restoration*, Comput. Appl. Math. 40, 239 (2021).

[11] Halilu, A.S. Majumder, A. Waziri, M.Y. and Ahmed, K. *Signal recovery with convex constrained nonlinear monotone equations through conjugate gradient hybrid approach*, Math. comput. Simulation, http://doi.org/10.1016/j.matcom.2021.03.020. (2021).

[12] Halilu, A.S. Majumder, A. Waziri, M.Y. Ahmed, K. and Awwal, A.M. *Motion control of the two joint planar robotic manipulators through accelerated Dai-Liao method for solving system of nonlinear equatiions*, Eng. Comput. https://doi.org/10.1108/EC-06-2021-0317

[13] Hager, W.W. and Zhang, H. *A new conjugate gradient method with guranteed descent and an efficient line search*, SIAM J. Optim. 16 (2005), 170-192.

[14] Hestenes, M.R. and Stiefel, E.L. *Methods of conjugate gradients for solving linear systems*, J. Res. Nat. Bur. Standards, 49(1952), 409-436.

[15] Hively, G.A. *On a class of nonlinear integral equations arising in transport theory*, SIAM J. Numer. Anal. 9 (1978), 787-792.

[16] Ibrahim, A.H. Deepho, J. Abubakar, A.B. Aremu, K.O. *A Modified Liu-Storey-conjugate descent hybrid projection method for convex constrained nonlinear equations and image restoration*, Numer. Alg. Cont. Optim. doi:10.3934/naco.2021022.

[17] Kelly, C. *Iterative methods for optimization*, Frontiers Appl. Math. 1999, DOI:10.1137/1.9781611970920 Corpus ID: 123596970.

[18] Koorapetse, M. Kaelo, P. *An efficient hybrid conjugate gradient-based projection method for convex constrained nonlinear monotone equations*, J. inter. math. 22 (6)(2019), 1031-1050.

[19] La Cruz, W. Martínez, J.M. and Raydan, M. *Spectral residual method without gradient information for solving large-scale nonlinear systems*, Theory and Experiments, Citeseer, Technical Report RT-04-08(2004).

[20] La Cruz, W. *A Spectral algorithm for large-scale systems of nonlinear monotone equations*, Numer. Algor. DOI 10.1007/s1107s-017-0299-8. (2017).

[21] Li, X. Shi, J. Dong, X. and Yu, J. *A new conjugate gradient method based on Quasi–Newton equation for unconstrained optimization*, J. Comput. Appl. Math. https://doi.org/10.1016/j.cam.2018.10.035

[22] Liu, Y. and Storey, C. *Efficient generalized conjugate gradient algorithms*, Part 1: Theory, J. Optim. Theory Appl. 69(1991), 129-137.

[23] Liu, J.K. and Li, S.J. *A projection method for convex constrained monotone nonlinear equations with applications*, Comput. Math. Appl. 70(10)(2015), 2442-2453.

[24] Meintjes, K. and Morgan, A.P. *A methodology for solving chemical equilibrium systems*, Appl. Math. Comput. 22(1987), 333-361.

[25] Mompati, S. and Kaelo, P. *Globally convergent three-term conjugate gradient projection methods for solving nonlinear monotone equations*, Arab. J. Math. 7(2018), 289-301.

[26] Muhammad, L. and Waziri, M.Y. *An Alternative three-term conjugate gradient algorithm for systems of nonlinear equations*, Intern. J. Math. Model. Comput. 07(02)(2017),145-157.

[27] Nakamura, W. Narushima, Y. and Yabe, H. *Nonlinear conjugate gradient methods with sufficient descent properties for unconstrained optimization.*, J. Ind. Manag. Optim. 9(3)(2013),595-619.

[28] Pang, J.S. *Inexact Newton methods for the nonlinear complementarity problem*, Math. Program. 36 (1986), 54-71.

[29] Polak, E. and Ribiére, G. *Note Sur la convergence de directions conjugèes*, Rev. Francaise Informat. Recherche Operationelle, 3e Annèe, 16 (1969), 35-43.

[30] Polyak, B.T. *The conjugate gradient method in extreme problems*, USSR Comp. Math. Math. Phys. 9 (1969), 94-112.

[31] Sabi'u, J. Shah, A. Waziri, M.Y. and Ahmed, K. *Modified Hager-Zhang conjugate gradient methods via singular value analysis for solving monotone nonlinear equations with convex constraint*, Int. J. Comput. Methods. hppt://doi.org/10.1142/S0219876220500437 (2020).

[32] Solodov, M.V. and Svaiter, B.F. *A globally convergent inexact Newton method for systems of monotone equations*, in: Reformulation: Nonsmooth, Piecewise Smooth, Semismooth and Smoothing Methods, Kluwer Academic Publishers, 1998, pp. 355-369.

[33] Sugiki, K. Narushima, Y. and Yabe, H. *Globally convergent three-term conjugate gradient methods that use secant conditions and generate descent search directions for unconstrained optimization*, J. Optim. Theory Appl. 153(2012), 733-757.

[34] Wang, C. Wang, Y. and Xu, C. *A projection method for a system of nonlinear monotone equations with convex constraints*, Math. Methods Oper. Res. 66(1)(2007), 33-46.

[35] Wang, X.Y. Li, X.J. and Kou, X.P. *A self-adaptive three-term conjugate gradient method for monotone nonlinear equations with convex constraints*, Calcolo DOI 10.1007/s10092-015-0140-5.

[36] Wang, Z. Li, P. Li, X. and Pham, H. *A modified three-term type CD conjugate gradient algorithm for unconstrained optimization problems*, Hindawi Mathematical Problems in Engineering Volume 2020, Article ID 4381515, 14 pages https://doi.org/10.1155/2020/4381515.

[37] Waziri, M.Y. Ahmed, K. and Sabi'u, J. *A family of Hager-Zhang conjugate gradient methods for system of monotone nonlinear equations*, Appl. Math. Comput. 361(2019), 645-660.

[38] Waziri, M.Y. Ahmed, K. and Sabi'u, J. *A Dai-Liao conjugate gradient method via modified secant equation for system of nonlinear equations*, Arab. J. Math. 9(2020), 443-457.

[39] Waziri, M.Y. Ahmed, K. and Sabi'u, *Descent Perry conjugate gradient methods for systems of monotone nonlinear equations*, Numer. Algor. 85(2020), 763-785.

[40] Waziri, M.Y. Ahmed, K. Sabi'u, J. and Halilu, A.S. *Enhanced Dai-Liao conjugate gradient methods for systems of monotone nonlinear equations*, SeMA J. 78(2020), 15-51.

[41] Waziri, M.Y. Usman, H. Halilu, A.S. and Ahmed, K. *Modified matrix-free methods for solving systems of nonlinear equations*, Optimization. 70(2021), 2321-2340

[42] Waziri, M.Y. and Ahmed, K. *Two descent Dai-Yuan conjugate gradient methods for systems of monotone nonlinear equations*, J. Sci. Comput. (2022) 90:36. https://doi.org/10.1007/s10915-021-01713-7.

[43] Waziri, M.Y. Ahmed, K. Halilu, A.S. Awwal, A.M. *Modified Dai-Yuan iterative scheme for nonlinear systems and its Application*, Numer. Alg. Control Optim. doi:10.3934/naco.2021044.

[44] Waziri, M.Y. Ahmed, K. and Halilu, A.S. *Adaptive three-term family of conjugate residual methods for system of monotone nonlinear equations*, Sao Paulo J. Math. Sci. https://doi.org/10.1007/s40863-022-00293-0

[45] Xiao, Y. Wang, Q. and Hu, Q. *Non-smooth equations based method for l1-norm problems with applications to compressed sensing*, Nonlinear Anal. Theory Methods Appl. 74(11)(2011), 3570-3577.

[46] Xiao, Y. and Zhu, H. *A conjugate gradient method to solve convex constrained monotone equations with applications in compressive sensing*, J. Math. Anal. Appl. 405(1)(2013), 310-319.

[47] Yuan, G. *Modified nonlinear conjugate gradient methods with sufficient descent property for large-scale optimization problems*, Optim. Lett. 3(2009), 11-21.

How to cite this article

Kiri, A.I., Waziri, M.Y. and Ahmed, K., A modified Liu-Storey scheme for nonlinear systems with an application to image recovery. *Iran. j. numer. anal. optim.*, 2023; 13(1): 38-58. https://doi.org/10.22067/ijnao.2022.75413.1107.